Received: 19 June 2021 | Revised: 21 September 2021 | Accepted: 21 October 2021

DOI: 10.1111/cas.15187

ORIGINAL ARTICLE

Cancer Science WILEY

Merkel cell polyomavirus–negative Merkel cell carcinoma is associated with JAK-STAT and MEK-ERK pathway activation

Takeshi Iwasaki[1] | Kazuhiko Hayashi[2] | Michiko Matsushita[2,3] | Daisuke Nonaka[4] | Kenichi Kohashi[1] | Satoshi Kuwamoto[2] | Yoshihisa Umekita[2] | Yoshinao Oda[1]

[1]Department of Anatomic Pathology, Graduate School of Medical Sciences, Kyushu University, Fukuoka, Japan

[2]Department of Pathology, School of Medicine, Faculty of Medicine, Tottori University, Yonago, Tottori, Japan

[3]Department of Pathobiological Science and Technology, School of Health Science, Faculty of Medicine, Tottori University, Yonago, Tottori, Japan

[4]Department of Cellular Pathology, The Guy's and St. Thomas' NHS Foundation Trust, London, UK

Correspondence
Yoshinao Oda, Department of Anatomic Pathology, Graduate School of Medical Sciences, Kyushu University, 3-1-1 Maidashi, Higashi-ku, Fukuoka 812-8582, Japan.
Email: oda.yoshinao.389@m.kyushu-u.ac.jp

Funding information
This work was supported by the Fukuoka Foundation for Sound Health Cancer Research through funding to [T.I.] and grants from the Japan Society for the Promotion of Science (No. 26460433 [K.H.] : 17K08720 [K.H.] 26860238 [M.M.] ; 17K15644 [M.M.] : 21K06885 [M.M.])

Abstract

Merkel cell polyomavirus (MCPyV) is monoclonally integrated into the genomes of approximately 80% of Merkel cell carcinomas (MCCs). While the presence of MCPyV affects the clinicopathological features of MCC, the molecular mechanisms of MCC pathogenesis after MCPyV infection are unclear. This study investigates the association between MCPyV infection and activation of the MEK-ERK and JAK-STAT signaling pathways in MCC to identify new molecular targets for MCC treatment. The clinicopathological characteristics of 30 MCPyV-positive and 20 MCPyV-negative MCC cases were analyzed. The phosphorylation status of MEK, ERK, JAK, and STAT was determined by immunohistochemical analysis. The activation status of the MEK-ERK and JAK-STAT pathways and the effects of a JAK inhibitor (ruxolitinib) was analyzed in MCC cell lines. Immunohistochemically, the expression of pJAK2 ($P = .038$) and pERK1/2 ($P = .019$) was significantly higher in MCPyV-negative than in MCPyV-positive MCCs. Male gender (hazard ratio [HR] 2.882, $P = .039$), older age (HR 1.137, $P < .001$), negative MCPyV status (HR 0.324, $P = .013$), and advanced cancer stage (HR 2.672, $P = .041$) were identified as unfavorable prognostic factors; however, the phosphorylation states of JAK2, STAT3, MEK1/2, and ERK1/2 were unrelated to the prognosis. The inhibition of cell proliferation by ruxolitinib was greater in MCPyV-negative MCC cell lines than in an MCPyV-positive MCC cell line. The expression of pERK1/2 and pMEK was higher in MCPyV-negative than in MCPyV-positive cell lines. These results suggest that activation of the JAK2 and MEK-ERK pathways was more prevalent in MCPyV-negative than in MCPyV-positive MCC and the JAK inhibitor ruxolitinib inhibited MEK-ERK pathway activation. Consequently, the JAK-STAT and MEK-ERK signaling pathways may be potential targets for MCPyV-negative MCC treatment.

KEYWORDS
JAK-STAT pathway, MEK-ERK pathway, Merkel cell carcinoma, Merkel cell polyomavirus

1 | INTRODUCTION

Merkel cell carcinoma (MCC) is a clinically aggressive neuroendocrine skin cancer that is associated with Merkel cell polyomavirus (MCPyV) in 80% of the cases.[1,2] MCPyV-positive MCCs harbor integrated, defective viral genomes that constitutively express viral oncogenes.[3] The features of MCC differ depending on MCPyV status in terms of morphology,[1] prognosis,[4-6] and molecular features, including UV-related genomic mutations[7] and activation of the phosphatidylinositol-3-kinase (PI3K)-Akt-mTOR[8,9] and Notch signaling pathways.[10] The Akt-mTOR signaling pathway provides cross talk between several signaling pathways, including JAK-STAT and MEK-ERK. JAK2 activation induces activation of several signaling pathways, including the transcription factor STAT3 and the mitogen-activated protein kinase (MAPK) pathway involving MEK and ERK kinase.[11]

The JAK-STAT and MEK-ERK signaling pathways play a multitude of important biological functions in both normal and malignant cells. Aberrant activation of these pathways has been observed in numerous cancers, including breast, lung, and head and neck carcinoma.[12] A previous study reported that pSTAT expression is associated with unfavorable outcomes in MCC.[13] The JAK-STAT signaling pathway can also directly mediate hepatitis B–driven Hepatocellular carcinoma tumorigenesis.[14] A recent study has shown that the trichodysplasia spinulosa polyomavirus (TSPyV) middle T antigen is involved in hyperactivation of the MEK-ERK-MNK1 signaling axis.[15] However, the association between MCPyV infection and activation of the JAK-STAT and MEK-ERK pathways in MCC remains to be clarified. In this study, we investigate the relationship between MCPyV infection and activation of the JAK-STAT and MEK-ERK pathways in MCC using next-generation genomic sequencing and immunohistochemical staining of clinical samples and an in vitro system of JAK inhibition to elucidate the molecular mechanisms underlying MCC pathogenesis.

2 | MATERIALS AND METHODS

2.1 | Patient specimens

This study was approved by the institutional review boards at Kyushu University (#2019-030) and Tottori University (#1216). The patient specimens were prepared as formalin-fixed, paraffin-embedded (FFPE) samples. We performed immunohistochemical staining of CK20 and neuroendocrine markers such as synaptophysin, chromogranin A, and CD56, and the histological diagnoses were reconfirmed by four pathologists (TI, DN, SK, and KH). We also confirmed the negative status for thyroid transcription factor-1 (TTF-1) to distinguish MCC from lung cancer metastases. MCPyV infection status was analyzed in the previous study using quantitative PCR and immunostaining using an antibody against MCPyV large T antigen (MCPyV-LT).[8] We used FFPE samples from 30 MCPyV-positive (Japan, 15 samples; United Kingdom, 15 samples) and 20 MCPyV-negative MCCs (Japan, 3 samples; United Kingdom, 17 samples) patients. Majority of the samples were used in our previous study,[8] and we newly added eight MCPyV-positive and two MCPyV-negative UK cases. Primary tumors were staged according to the latest American Joint Committee on Cancer (AJCC) staging system.[16] The patients include 18 males and 32 females, with the age at diagnosis ranging from 55 to 94 years old (average, 78 years). Of the 50 tumors analyzed, 47 were primary and three were metastatic. Resected specimen tumor sites included the head (21 cases), extremity (26 cases), trunk (one case), and lymph nodes (two cases). The average tumor size was 3.5 cm (range, 0.5-7.5 cm). AJCC tumor stages were as follows: stage I, 12 tumors; stage II, 27 tumors; stage III, eight tumors; stage IV, two tumors; and unknown, one tumor.

2.2 | Immunohistochemistry (IHC)

FFPE blocks were cut into 3-μm-thick slices, dewaxed in xylene, and rehydrated in a graded series of ethanol. Samples were treated with 3% hydrogen peroxide in methanol for 30 min to block endogenous peroxidase and washed twice with PBS. The sections were heated in 0.01 M citrate buffer (pH 6). The primary antibodies used in this study are listed in Table S1. Primary antibodies were detected using the Dako Envision+ System (Dako). The Dako Liquid DAB+ substrate chromogen system (Dako) served as the chromogen. Immunostaining was evaluated using a proportional expression score (PS) as follows: 0, no staining; 1, <1% stained; 2, 1-9%; 3, 10-32%; 4, 33-65%; and 5, ≥66%.

2.3 | DNA extraction, next-generation sequencing, and bioinformatics

For next-generation sequencing, we selected cases in which the number of samples required for analysis was sufficient. The total DNA was isolated from MCC cases using the GeneRead DNA FFPE kit (Qiagen). DNA quality was tested using a Bioanalyzer 2100 with the Agilent DNA 1000 kit (Agilent Technologies), and eight MCC cases (four MCPyV-positive; four MCPyV-negative) with sufficient DNA quality and concentration were selected. An amplicon library of the target exons was prepared according to the manufacturer's instructions using an Ion ampliseq Cancer hotspot panel v2 (Thermofisher) targeting 2790 cancer-related hotspots in 50 genes. The constructed libraries were sequenced using Ion Proton 410 (Thermofisher). After alignment, variants were called using the TSVC module of the Torrent Suite (Thermofisher) and annotated using the Ensembl Variant Effect Predictor.[17] Principal component analysis (PCA) was measured and visualized using the web-based software MuSiCa.[18]

2.4 | Statistical analysis for clinicopathological data

Clinicopathological parameters and immunohistochemical findings were analyzed based on the MCPyV status using the Wilcoxon or

Fisher exact test. Correlations among expression levels, as obtained in immunohistochemical analysis, were calculated using Spearman's rank correlation coefficient. Prognostic analysis was performed using the log-rank test with the Kaplan-Meier analysis. The goodness of fit of each Cox model was evaluated using the likelihood ratio test. Data were analyzed using the SPSS software (version 20.0 J, SPSS Japan). A *P*-value of <.05 was considered significant.

2.5 | Cell proliferation assay

The MCC cell lines were obtained from CellBank Australia and grown in RPMI 1640 supplemented with 10% fetal bovine serum. The cells were seeded in 96-well plates at a density of 3000 cells/well (MCC13 and MCC14/2) or 10 000 cells/well (MKL-1), incubated overnight, and then treated with the JAK inhibitor ruxolitinib (INCB018424) (5-500 μM) or vehicle DMSO. After 24, 48, 72, or 120 hours of incubation, cell viability was determined by WST-8 assay using a cell counting assay kit (Nacalai Tesque) according to the manufacturer's instructions. Absorbance was measured at 450 nm using a microplate absorbance reader (iMARK, Bio-Rad). Cell proliferation assay results were analyzed based on the JAK2 inhibitor concentration using Dunnett's multiple comparison test for comparison with the vehicle. Data were analyzed using the SPSS software (version 20.0 J, SPSS Japan). A *P* value of <.05 was considered significant.

2.6 | Western blot analysis

Cells were washed twice with PBS, centrifuged, resuspended in 2× sodium dodecyl sulfate (SDS) sample buffer, and then denatured at 97°C for 3 minutes as performed previously.[19] The supernatant of the lysate was separated via SDS-PAGE (4%-20% Mini-PROTEAN TGX gel, Bio-Rad) and electrotransferred to a polyvinylidene fluoride membrane (2.5 A, 25 V, 7 minutes) using the Trans-Blot Turbo Transfer System (Bio-Rad Laboratories). The membrane was blocked for 15 minutes in Blocking One-P (Nacalai Tesque) and incubated with primary antibodies in Hikari Solution A (Nacalai Tesque) followed by incubation with secondary antibodies and detection using Chemi-Lumi One Ultra (Nacalai Tesque). The primary antibodies used for Western blotting are summarized in Table S1.

3 | RESULTS

3.1 | Histological findings and IHC staining

Representative results of hematoxylin and eosin staining and immunohistochemical staining are shown in Figure 1. The results of immunostaining for the JAK-STAT pathway are summarized in Table 1. MCPyV-positive MCC cells (Figure 1A) presented as higher number of round-shaped nuclei and nuclear-cytoplasmic ratio than MCPyV-negative MCC cells (Figure 1B). MCPyV-LT expression was diffusely positive in the nuclei of MCPyV-positive MCC tumor cells (Figure 1C) and negative in those of MCPyV-negative MCC tumor cells (Figure 1D). Expressions of JAK2 phosphorylation at Tyr1007 and Tyr1008 (Figure 1E and F) and ERK1/2 phosphorylation at Thr202 and Tyr204 (Figure 1K and L) were significantly greater in MCPyV-negative MCC (Figure 1F and L) than in MCPyV-positive MCC (Figure 1E and K) ($P = .038$ and $P = .019$, respectively). Expression of MEK1/2 phosphorylated at Ser221 was significantly greater in MCPyV-positive MCC (Figure 1I) than in MCPyV-negative MCC (Figure 1J) ($P = .009$). STAT3 phosphorylation at Tyr705 was positive in both MCPyV-positive and -negative MCCs (Figure 1 G and H), but no significant difference was observed between MCPyV-positive and -negative MCCs. The mean expression score of MCC was 3.14 ± 1.48 (pJAK2), 1.64 ± 1.08 (pSTAT3), 1.10 ± 1.31 (pERK), and 3.42 ± 1.62 (pMEK). A correlation between pSTAT3 and pERK expression was present, albeit not significant ($P = .063$; $\rho = 0.265$).

3.2 | Gene mutation analysis

Variants in 36 loci of 21 genes were identified, including pathogenic mutations in the *PTPN11*, *TP53*, *RB1*, *SMAD4*, and *PIK3CA* genes (Figure 2A). No mutations in *JAK2* or *JAK3* were observed. PCA (Figure 2B) showed that PC1 and PC2 had variances of 36.7% and 23.2%, respectively and that MCPyV-negative and MCPyV-positive MCCs were separated by PC1 and PC2. The number of single-nucleotide variants (SNVs) is shown in Figure 2C. The average number of SNV was 14 (range, 9-18). More SNVs were observed in MCPyV-negative MCC than in MCPyV-positive MCC (average, 15.3 vs. 13.2, respectively), but without statistical significance ($P = .465$, Wilcoxon test) (Figure 2C). MCPyV-positive cases had more T > A variants, but without statistical significance (Figure 2D). Grouping of SNVs by trinucleotide context showed that C > T substitutions at dipyrimidines were predominant (Figure 2E).

3.3 | Prognostic factors

Follow-up information was available for patients; the average follow-up period after surgery was 22 months (range, 1-72 months). No cases were treated with immune checkpoint inhibitors. Results of survival analysis using the Kaplan-Meier method and log-rank test are summarized in Figure 3. Higher pSTAT3 expression was associated with favorable outcomes, but this relationship was not significant (overall survival [OS], $P = .417$). Log-rank test results show that the expressions of pJAK2, pERK, and pMEK were not associated with prognosis. Univariate Cox proportional hazard analyses showed that male sex, old age, negative MCPyV status, and advanced stage were unfavorable prognostic factors (Table 2). Cox proportional hazard analysis also showed no relationship between phosphorylation of JAK2, STAT3, MEK1/2, and ERK1/2 and prognosis (Table 2).

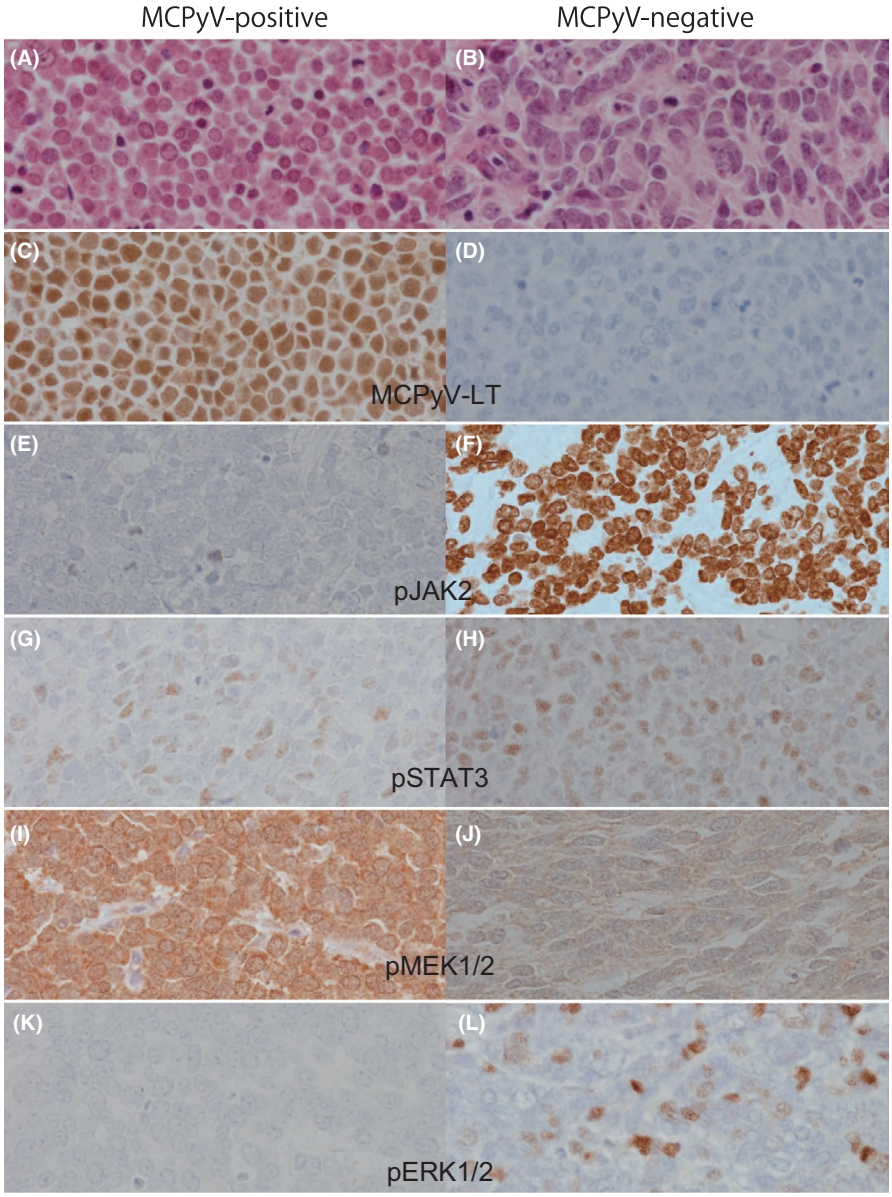

FIGURE 1 Representative immunostaining of JAK-STAT pathway proteins in Merkel cell polyomavirus (MCPyV)-positive and -negative Merkel cell carcinomas (MCCs). MCPyV-positive MCCs: A, C, E, G, I, and K. MCPyV-negative MCCs: B, D, F, H, J, and L. A and B, MCPyV-positive MCC cells (A) showed more round shape nuclei and higher nuclear-cytoplasmic ratio than did MCPyV-negative MCC cells (B). C and D, Strong, diffuse nuclear immunoreactivity for MCPyV large T antigen (MCPyV-LT) was observed in samples positive for MCPyV DNA (C) but not in those without MCPyV DNA (D). E and F, pJAK2 staining of nuclei was observed significantly more frequently in MCPyV-negative MCC (F) than in MCPyV-positive MCC (E) ($P = .038$). G and H, No significant differences were observed in p-STAT3 signal activation status between MCPyV-positive and -negative MCCs. I and J, pMEK1/2 staining of nuclei was higher in MCPyV-positive MCC (I) than MCPyV-negative MCC (J). K and L, pERK1/2 nuclear staining was significantly higher in MCPyV-negative MCC (L) than MCPyV-negative MCC (K)

3.4 | Cell proliferation assay

To investigate the functional role of pJAK2 in MCC, MCPyV-negative MCC cell lines (MCC13 and MCC14/2) and a MCPyV-positive MCC cell line (MKL-1) were treated with the JAK inhibitor ruxolitinib. At a concentration ≥50 μM, ruxolitinib significantly inhibited cell proliferation in all cell lines (Figure 4), with greater inhibition observed in the MCC13 and MCC14/2 cell lines than in MKL-1 (Figure 4B).

3.5 | Western blot analysis

The expression of JAK-STAT and MEK-ERK pathway proteins was assessed by Western blot analysis in MCC cell lines treated with a JAK inhibitor ruxolitinib for 3 days (Figure 4C and Figure S1). The representative data of patients treated with JAK inhibitor for 48 hours are shown in Figure 4C. The MCPyV-negative cell lines (MCC13 and MCC14/2) expressed higher levels of pMEK and pERK1/2 than the MCPyV-positive cell line (MKL-1) (Figure 4C). Ruxolitinib, at a concentration of 50 μM, decreased pMEK expression in the MKL-1 cell line and temporarily in the MCC14/2 cell line, but increased expression in the MCC14/2 cell line after 2 and 3 days (Figure S1). Elevated expression of pERK1/2 was inhibited by ruxolitinib in MCC13 and MCC14/2, but not in MKL-1 cells (Figure 4C). pSTAT3 expression was higher in MCC14/2 than in MCC13 or MKL-1 cells, and this pSTAT3 overexpression was not altered by ruxolitinib treatment in MCC13 cells (Figure 4C). JAK inhibition resulted in dose-dependent STAT3 inactivation in MKL-1 cells, but not in MCC13 cells (Figure 4C). Notably, treatment with JAK inhibitor at 5 μM concentration for 1 day markedly increased the pSTAT3 level (Figure S1). pSTAT1 expression was increased in MCC 14/2 cells treated with 5μM ruxolitinib at day 1 (Figure S1). STAT1 expression was decreased by 50 μM ruxolitinib treatment in the MCC13 and MCC14/2 cell lines (Figure 4C).

TABLE 1 Comparison of clinicopathological parameters of Merkel cell carcinomas based on Merkel cell polyomavirus status

Clinicopathological parameters	MCPyV-positive	MCPyV-negative	*P*-value
Age (yo), mean ± SD	75.6 ± 8.2	81.2 ± 9.2	.052
Sex (male/female)	11/19	7/13	.904
AJCC stage (I, II/ III, IV)	24/6	14/6	.506
Race (Asian/Caucasoid)	15/15	3/17	.016*
p-JAK2 proportion score, mean ± SD	2.80 ± 1.42	3.65 ± 1.46	.038*
p-STAT3 proportion score, mean ± SD	1.73 ± 1.01	1.50 ± 1.19	.572
p-MEK1/2 proportion score, mean ± SD	3.87 ± 1.48	2.75 ± 1.62	.009*
p-ERK1/2 proportion score, mean ± SD	0.77 ± 1.25	1.60 ± 1.27	.019*

Abbreviations: AJCC Stage, American Joint Committee on Cancer Staging System 8th ed.; MCPyV, Merkel cell polyomavirus; SD, standard deviation; yo, years old.

*Statistically significant ($P < .05$).

4 | DISCUSSION

In this study, we demonstrated frequent activation of the JAK-STAT and MEK-ERK signaling pathways in MCPyV-negative MCC resected specimens and MCPyV-negative cell lines and showed a significantly higher activation rate of pJAK2 ($P = .038$) and pERK ($P = .019$) in MCPyV-negative MCCs than in MCPyV-positive MCCs. We and others have shown clinicopathological differences between MCPyV-positive and MCPyV-negative MCC.[1,4,8,10,20] Histologically, MCPyV-positive MCC tumor cells had uniform round nuclei and little cytoplasm, whereas MCPyV-negative tumor cells had irregular nuclei and abundant cytoplasm.[1] Patients with MCPyV-positive MCC had more favorable outcomes than did those with MCPyV-negative MCC.[4-6,21] In addition, Akt phosphorylation at T308 was significantly greater in MCPyV-negative than in MCPyV-positive MCCs.[8] These results suggested that MCC pathogenesis differs depending on MCPyV status. In this study, clinical sample analysis revealed that the JAK-STAT and MEK-ERK signaling pathways are activated more frequently in MCPyV-negative MCC than in MCPyV-positive MCC. Activation of the JAK-STAT[22] and MEK-ERK[23] pathway is often observed in some cancers, including bladder carcinoma, malignant glioma, and hepatocellular carcinoma. Immunostaining of MCC clinical samples showed that MCPyV-negative MCCs expressed higher levels of pERK and lower levels of pMEK than did MCPyV-positive MCCs. The ERK1/2-MAP pathway is involved in numerous negative feedback loops by inhibiting the phosphorylation of MEK1/2 and Raf.[24] Our results suggest that the MEK-ERK pathway is activated in MCPyV-negative MCCs, resulting in activated ERK (pERK) suppressing MEK phosphorylation. A previous study, performed (2006) when MCPyV had not yet been discovered, reported that the classic RAS/Raf/MEK-ERK pathway is inactivated in MCC.[25] However, the fact that most MCCs (approximately 80%) are MCPyV positive is noteworthy. We observed MEK-ERK activation in MCPyV-negative patients, which represented only 20% of the MCC cases; thus, differing results regarding activation of this pathway may result from differences in the MCPyV status. In addition, IHC results of clinical samples revealed higher levels of pJAK2 in MCPyV-negative MCC than in MCPyV-positive MCC; however, the pSTAT3 expression level was not significantly different between MCPyV-positive and -negative MCC. These results suggest that STAT3 in MCPyV-positive cases is activated via other molecules, such as JAK1, or due to the effect of the activated MEK-ERK pathway cross talk.

PCA of next-generation genomic sequencing showed differences in the mutation pattern between MCPyV-positive and -negative MCC. Pathogenic mutations in *TP53*, *RB1*, *BAP1*, *PIK3CA*, *AKT1*, and *EZH2* genes have been reported in MCC,[26] and MCPyV-negative MCC has a high mutation burden characterized by a predominance of UV signature mutations with recurrent inactivation of tumor suppressor genes such as TP53, RB1, and NOTCH.[4,7,27-29] This study confirms the presence of pathogenic mutations in *TP53* in MCPyV-positive and MCPyV-negative MCCs and *PIK3CA* in MCPyV-negative MCC. In addition, we observed more frequent genomic variants in MCPyV-negative than in MCPyV-positive MCC, but this difference was not statistically significant. The UV signature mutation (C > T in dipyrimidines) was also observed, but the probability of such mutation was independent of MCPyV status. Because we used target DNA sequencing from a cancer panel in this study, these controversial results might result from limited sequence lengths and the small number of samples tested. In addition, differences in UV damage susceptibility due to racial differences, such as Asians and Caucasians, may also influence the results. Activating mutations in *JAK*s or other upstream oncogenes are known to activate the JAK-STAT pathway in hematopoietic diseases such as polycythemia vera and essential thrombocytosis.[30] However, we observed no mutations in the *JAK2* or *JAK3* gene in any of the eight analyzed cases.

Prognostic factor analysis reconfirmed the MCPyV-negative status was associated with unfavorable outcomes, as indicated in our and other previous studies.[4,21] Advanced AJCC stage is also an unfavorable prognostic factor, as previously reported.[31] Activated STAT3 positively correlates with a better prognosis in patients with colorectal carcinoma, leiomyosarcoma, and nasopharyngeal carcinoma.[32-34] In our study, Kaplan-Meier analysis showed that patients with higher STAT3 expression had more favorable outcomes than did those with lower expression; however, this difference was not statistically significant. The other immunohistochemical markers related to the JAK-STAT or MEK-ERK pathway were not related to prognosis.

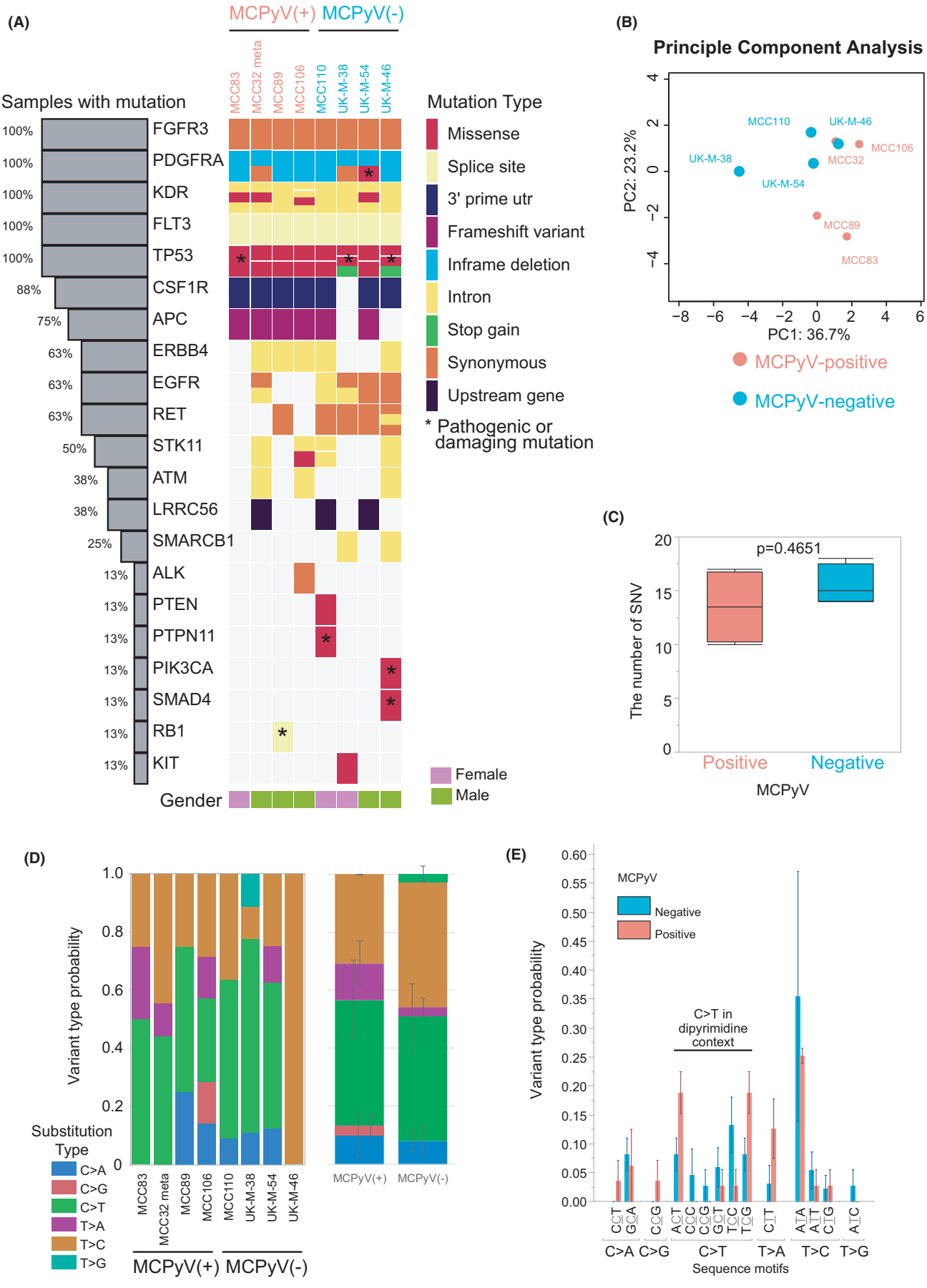
(A)
MCPyV(+) MCPyV(-)
MCC83
MCC32 meta
MCC89
MCC106
MCC110
UK-M-38
UK-M-54
UK-M-46
Samples with mutation
100% FGFR3
100% PDGFRA
100% KDR
100% FLT3
100% TP53
88% CSF1R
75% APC
63% ERBB4
63% EGFR
63% RET
50% STK11
38% ATM
38% LRRC56
25% SMARCB1
13% ALK
13% PTEN
13% PTPN11
13% PIK3CA
13% SMAD4
13% RB1
13% KIT
Gender
Mutation Type
Missense
Splice site
3' prime utr
Frameshift variant
Inframe deletion
Intron
Stop gain
Synonymous
Upstream gene
* Pathogenic or damaging mutation
Female
Male
(B)
Principle Component Analysis
PC2: 23.2%
PC1: 36.7%
MCC110
UK-M-46
MCC106
UK-M-38
MCC32
UK-M-54
MCC89
MCC83
MCPyV-positive
MCPyV-negative
(C)
p=0.4651
The number of SNV
Positive
Negative
MCPyV
(D)
Variant type probability
Substitution Type
C>A
C>G
C>T
T>A
T>C
T>G
MCC83
MCC32 meta
MCC89
MCC106
MCC110
UK-M-38
UK-M-54
UK-M-46
MCPyV(+) MCPyV(-)
MCPyV(+)
MCPyV(-)
(E)
Variant type probability
MCPyV
Negative
Positive
C>T in dipyrimidine context
C>A C>G C>T T>A T>C T>G
Sequence motifs

FIGURE 2 Summary of gene mutation analysis. A, Commutation plot of Merkel cell polyomavirus (MCPyV)-positive and -negative Merkel cell carcinoma (MCC) tissues showing a variety of mutations, including pathogenic or likely pathogenic mutations (*). Single columns represent individual patients. Samples are grouped according to MCPyV status, as indicated in the first row, and the sex is indicated in the bottom row. B, Principal component analysis (PCA) of signature across patients (PCA on signature-specific variants per patient). Points are colored according to MCPyV status. *X*-axis and *Y*-axis denote PC1 and PC2, respectively. PC1, first principal component; PC2, second principal component. MCPyV-negative and -positive MCCs were separated by PC1 (36.7%) and PC2 (23.2%). C, Bar plot indicating the number of single-nucleotide variants (SNVs). No statistically significant difference in the number of SNVs was observed between the MCPyV-positive and -negative MCCs ($P = .4651$). D, Bar plot indicating the SNV probability of each MCC sample. C > T substitution is predominant in both MCPyV-positive and -negative cases. The probability of C > T substitution did not differ between MCPyV-negative and -positive MCC. E, Trinucleotide signature for included SNVs shows mutations primarily at dipyrimidines, characteristic of mutations arising from UV photoproduct formation (C > T in dipyrimidine context)

FIGURE 3 Prognostic analysis. Overall survival (OS) stratified by pJAK2, pSTAT3, pMEK, and pERK1/2 expression status. Higher pSTAT3 expression was associated with favorable outcomes, but the relationship was not significant (log-rank test, $P = .417$). The expression of pJAK2, pMEK, and pERK1/2 were not associated with prognosis. PS, proportional expression score

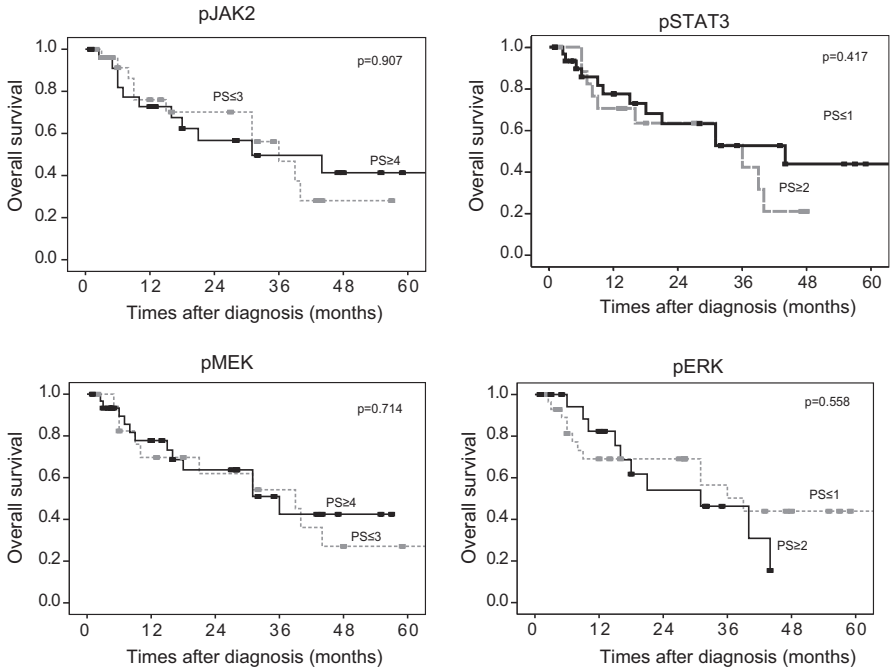

TABLE 2 Univariate Cox regression analyses of the relationships of overall survival with clinicopathological factors and immunohistochemical results

Univariate	HR	95% CI	*P*-value
Sex (male/female)	2.882	1.052-7.893	.039*
Age	1.137	1.062-1.218	<.001*
MCPyV (positive/negative)	0.324	0.133-0.787	.013*
Stage (III, IV/I, II)	2.672	1.043-6.846	.041*
p-JAK2	0.940	0.688-1.284	.697
p-STAT3	0.889	0.592-1.335	.570
p-MEK1/2	0.925	0.731-1.171	.519
p-ERK1/2	1.080	0.772-1.512	.653

Abbreviations: CI, confidence interval; HR, hazard ratio; MCPyV, Merkel cell polyomavirus.
*$P < 0.05$.

MCC cell line analysis revealed that MCPyV-negative cell lines exhibited greater MEK-ERK pathway activation than did MCPyV-positive cells. Treatment with the JAK inhibitor ruxolitinib inhibited this MEK-ERK pathway activation in MCC-negative cell lines. JAK2 phosphorylation and dimerization initiate processes that promote cell proliferation and survival, resulting in increased expression of transcription factors STAT3 and STAT5 and the activated PI3K/AKT pathway and MAPK pathway involving MEK and ERK kinases.[11] The JAK1/JAK2 inhibitor ruxolitinib is used in treating patients with symptomatic myelofibrosis and polycythemia vera.[35] Previous studies also report that ruxolitinib inhibits the phosphorylation of ERK1/2 in the MEK-ERK pathway.[36,37] Our results may confirm that ruxolitinib inhibits pERK1/2 in MCPyV-negative cell lines and that its inhibition of MCC proliferation is greater in MCPyV-negative than MCPyV-positive MCC. These results indicate that the proliferation of MCPyV-negative MCC depends not only on the JAK-STAT pathway but also on the MEK-ERK pathway. In contrast, pSTAT3 is inhibited by ruxolitinib in the MCPyV-positive cell line and is activated in MCPyV-negative cell lines. These findings could be explained by the induction of negative feedback loops of the JAK-STAT pathway in MCPyV-negative cell lines. As for the limitations of the current investigation, MCC is extremely rare; thus, the number of commercially available MCC cell lines is limited. Therefore, further investigation such as dual inhibition of the JAK-STAT and MEK-ERK pathways using more MCC line types or MCC primary cell culture is desired.

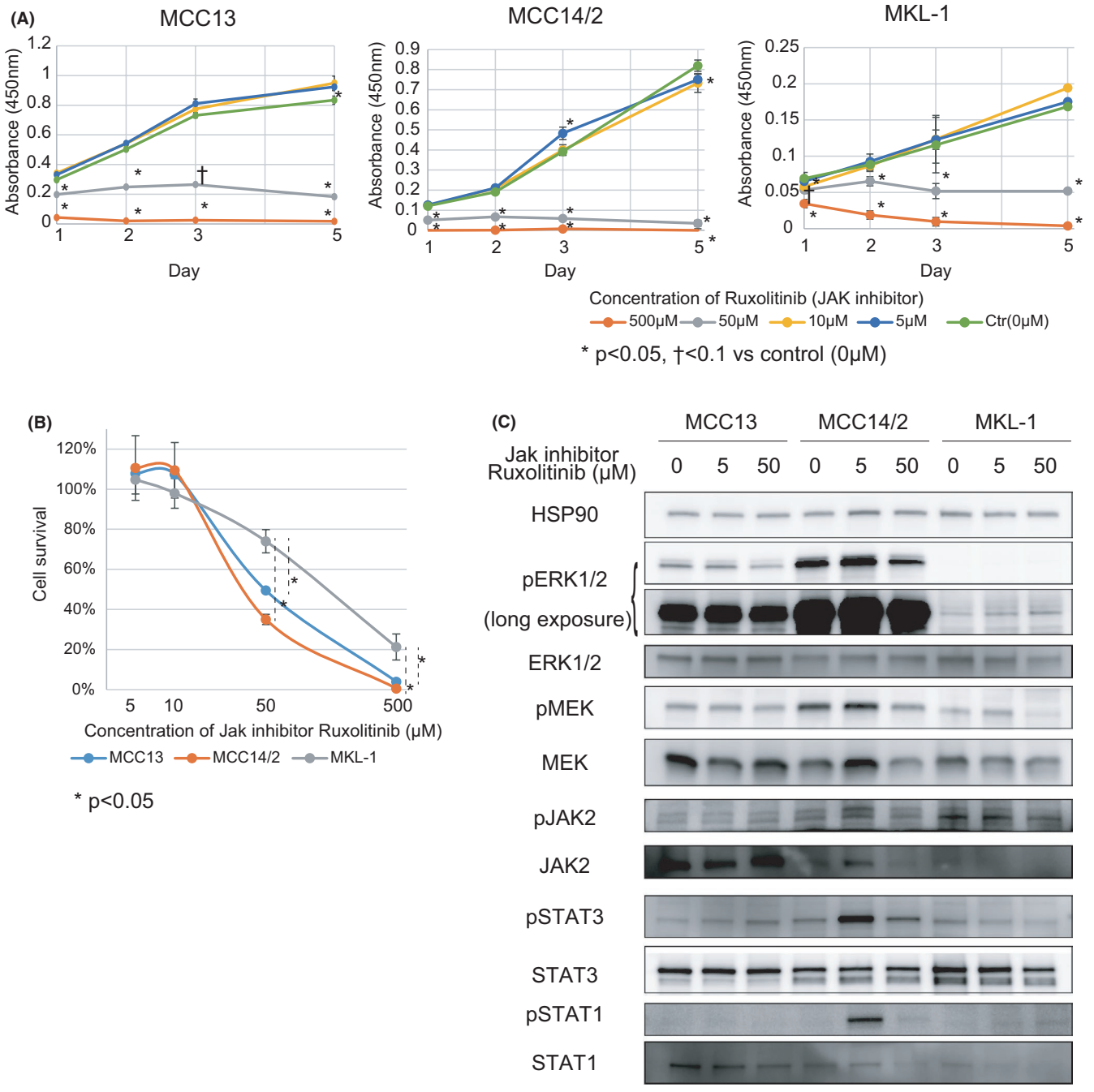

FIGURE 4 The JAK1/2 inhibitor ruxolitinib inhibited Merkel cell carcinoma (MCC) proliferation in vitro. A, Cell viability was confirmed by WST-8 assay in Merkel cell polyomavirus (MCPyV)-negative cell lines (MCC13 and MCC14/2) and the MCPyV-positive cell line (MKL-1) treated with ruxolitinib or vehicle alone (DMSO). Ruxolitinib treatment (≥50 μM) significantly inhibited cell proliferation in all cell lines (*$P < .05$; †$P < .1$). B, Ruxolitinib (50 μM and 500 μM) inhibition of cell proliferation was greater in MCPyV-negative than -positive cells. A and B, Each bar represents the mean ± SD. C, JAK-STAT and MEK-ERK pathway activity was examined by Western blot assay. JAK1/2 inhibitor ruxolitinib (50 μM) inhibited the phosphorylation of ERK1/2 in MCC13 and MCC14/2 cells (MCPyV-negative cell lines), but not in MKL-1 cells (MCPyV-positive cell line)

In addition, the concentration of ruxolitinib used in this cell line experiment (ie, 50 μM) is higher than the plasma concentration of ruxolitinib when the FDA-approved therapeutic dose of ruxolitinib is administered to humans. To confirm our data, further investigation using MCC mouse xenograft models, treated with JAK-STAT and MEK-ERK inhibitors, are warranted.

In conclusion, we observed that activation of the JAK2 and MEK-ERK pathways was more prevalent in MCPyV-negative MCC than in MCPyV-positive one. Therefore, MCC tumorigenic pathways may differ depending on MCPyV status. In vitro, the JAK inhibitor ruxolitinib was shown to inhibit MEK-ERK pathway activation, particularly in MCPyV-negative MCC. Thus, JAK-STAT and MEK-ERK pathway

inhibition may present a promising new treatment strategy for patients with advanced MCPyV-negative MCC.

ACKNOWLEDGMENTS

We thank the Research Initiative Center at Tottori University for technical assistance and the Research Support Center Graduate School of Medical Sciences at Kyushu University for providing equipment. We appreciate the English language review by Enago and thank Mr H. Sugihara and Dr K. Adachi at Tottori University and Mrs M. Nakamizo and Mrs M. Tomita at Kyushu University for technical assistance. We would also like to thank Dr I. Kinoshita and Dr H. Yamamoto at Kyushu University Hospital and Dr T. Iwasaki at Yamagishi Internal Medicine Clinic for helpful discussion. Part of this work was presented at the 110th USCAP annual meeting.

CONFLICT OF INTEREST

All authors declare that they have no conflict of interests.

ORCID

Takeshi Iwasaki https://orcid.org/0000-0001-5277-2932
Yoshinao Oda https://orcid.org/0000-0001-9636-1182

REFERENCES

1. Kuwamoto S, Higaki H, Kanai K, et al. Association of Merkel cell polyomavirus infection with morphologic differences in Merkel cell carcinoma. *Hum Pathol*. 2011;42:632-640.
2. Feng H, Shuda M, Chang Y, Moore PS. Clonal integration of a polyomavirus in human Merkel cell carcinoma. *Science*. 2008;319:1096-1100.
3. Czech-Sioli M, Gunther T, Therre M, et al. High-resolution analysis of Merkel Cell Polyomavirus in Merkel Cell Carcinoma reveals distinct integration patterns and suggests NHEJ and MMBIR as underlying mechanisms. *PLoS Pathog*. 2020;16:e1008562.
4. Higaki-Mori H, Kuwamoto S, Iwasaki T, et al. Association of Merkel cell polyomavirus infection with clinicopathological differences in Merkel cell carcinoma. *Hum Pathol*. 2012;43:2282-2291.
5. Bhatia K, Goedert JJ, Modali R, Preiss L, Ayers LW. Immunological detection of viral large T antigen identifies a subset of Merkel cell carcinoma tumors with higher viral abundance and better clinical outcome. *Int J Cancer*. 2010;127:1493-1496.
6. Sihto H, Kukko H, Koljonen V, Sankila R, Bohling T, Joensuu H. Merkel cell polyomavirus infection, large T antigen, retinoblastoma protein and outcome in Merkel cell carcinoma. *Clin Cancer Res*. 2011;17:4806-4813.
7. Wong SQ, Waldeck K, Vergara IA, et al. UV-associated mutations underlie the etiology of MCV-negative Merkel cell carcinomas. *Can Res*. 2015;75:5228-5234.
8. Iwasaki T, Matsushita M, Nonaka D, et al. Comparison of Akt/mTOR/4E-BP1 pathway signal activation and mutations of PIK3CA in Merkel cell polyomavirus-positive and Merkel cell polyomavirus-negative carcinomas. *Hum Pathol*. 2015;46:210-216.
9. Nardi V, Song Y, Santamaria-Barria JA, et al. Activation of PI3K signaling in Merkel cell carcinoma. *Clin Cancer Res*. 2012;18:1227-1236.
10. Wardhani LO, Matsushita M, Kuwamoto S, et al. Expression of Notch 3 and Jagged 1 Is associated with Merkel cell polyomavirus status and prognosis in Merkel cell carcinoma. *Anticancer Res*. 2019;39:319-329.
11. Meyer SC, Levine RL. Molecular pathways: molecular basis for sensitivity and resistance to JAK kinase inhibitors. *Clin Cancer Res*. 2014;20:2051-2059.
12. Sansone P, Bromberg J. Targeting the interleukin-6/Jak/stat pathway in human malignancies. *J Clin Oncol*. 2012;30:1005-1014.
13. Gonzalez-Vela MDC, Curiel-Olmo S, Derdak S, et al. Shared oncogenic pathways implicated in both virus-positive and UV-induced Merkel cell carcinomas. *J Invest Dermatol*. 2017;137:197-206.
14. Lee YH, Yun Y. HBx protein of hepatitis B virus activates Jak1-STAT signaling. *J Biol Chem*. 1998;273:25510-25515.
15. Wu JH, Narayanan D, Simonette RA, Rady PL, Tyring SK. Dysregulation of the MEK/ERK/MNK1 signalling cascade by middle T antigen of the trichoydsplasia spinulosa polyomavirus. *J Eur Acad Dermatol Venereol* 2017;31:1338-1341.
16. Amin MB, American Joint Committee on Cancer. *AJCC Cancer Staging Manual*, 8th edn; xvii, 1024 pages.
17. McLaren W, Gil L, Hunt SE, et al. The ensembl variant effect predictor. *Genome Biol*. 2016;17:122.
18. Diaz-Gay M, Vila-Casadesus M, Franch-Exposito S, Hernandez-Illan E, Lozano JJ, Castellvi-Bel S. Mutational Signatures in Cancer (MuSiCa): a web application to implement mutational signatures analysis in cancer samples. *BMC Bioinformatics*. 2018;19:224.
19. Harada A, Maehara K, Ono Y, et al. Histone H3.3 sub-variant H3mm7 is required for normal skeletal muscle regeneration. *Nat Commun*. 2018;9:1400.
20. Kuromi T, Matsushita M, Iwasaki T, et al. Association of expression of the hedgehog signal with Merkel cell polyomavirus infection and prognosis of Merkel cell carcinoma. *Hum Pathol*. 2017;69:8-14.
21. Moshiri AS, Doumani R, Yelistratova L, et al. Polyomavirus-negative Merkel cell carcinoma: a more aggressive subtype based on analysis of 282 cases using multimodal tumor virus detection. *J Invest Dermatol*. 2017;137:819-827.
22. Hin Tang JJ, Hao Thng DK, Lim JJ, Toh TB. JAK/STAT signaling in hepatocellular carcinoma. *Hepatic Oncology*. 2020;7:HEP18.
23. Lorentzen HF. Targeted therapy for malignant melanoma. *Curr Opin Pharmacol*. 2019;46:116-121.
24. Lake D, Correa SA, Muller J. Negative feedback regulation of the ERK1/2 MAPK pathway. *Cell Mol Life Sci*. 2016;73:4397-4413.
25. Houben R, Michel B, Vetter-Kauczok CS, et al. Absence of classical MAP kinase pathway signalling in Merkel cell carcinoma. *J Invest Dermatol*. 2006;126:1135-1142.
26. Harms PW, Collie AM, Hovelson DH, et al. Next generation sequencing of Cytokeratin 20-negative Merkel cell carcinoma reveals ultraviolet-signature mutations and recurrent TP53 and RB1 inactivation. *Mod Pathol*. 2016;29:240-248.
27. Cimino PJ, Robirds DH, Tripp SR, Pfeifer JD, Abel HJ, Duncavage EJ. Retinoblastoma gene mutations detected by whole exome sequencing of Merkel cell carcinoma. *Mod Pathol*. 2014;27:1073-1087.
28. Harms PW, Vats P, Verhaegen ME, et al. The distinctive mutational spectra of polyomavirus-negative Merkel cell carcinoma. *Can Res*. 2015;75:3720-3727.
29. Goh G, Walradt T, Markarov V, et al. Mutational landscape of MCPyV-positive and MCPyV-negative Merkel cell carcinomas with implications for immunotherapy. *Oncotarget*. 2016;7:3403-3415.
30. O'Shea JJ, Schwartz DM, Villarino AV, Gadina M, McInnes IB, Laurence A. The JAK-STAT pathway: impact on human disease and therapeutic intervention. *Annu Rev Med*. 2015;66:311-328.
31. Harms KL, Healy MA, Nghiem P, et al. Analysis of prognostic factors from 9387 Merkel cell carcinoma cases forms the basis for the new 8th edition AJCC Staging System. *Ann Surg Oncol*. 2016;23:3564-3571.
32. Setsu N, Kohashi K, Endo M, et al. Phosphorylation of signal transducer and activator of transcription 3 in soft tissue leiomyosarcoma is associated with a better prognosis. *Int J Cancer*. 2013;132:109-115.
33. Gordziel C, Bratsch J, Moriggl R, Knosel T, Friedrich K. Both STAT1 and STAT3 are favourable prognostic determinants in colorectal carcinoma. *Br J Cancer*. 2013;109:138-146.

34. Hsiao JR, Jin YT, Tsai ST, Shiau AL, Wu CL, Su WC. Constitutive activation of STAT3 and STAT5 is present in the majority of nasopharyngeal carcinoma and correlates with better prognosis. *Br J Cancer*. 2003;89:344-349.
35. Vannucchi AM, Kiladjian JJ, Griesshammer M, et al. Ruxolitinib versus standard therapy for the treatment of polycythemia vera. *N Engl J Med*. 2015;372:426-435.
36. Stivala S, Codilupi T, Brkic S, et al. Targeting compensatory MEK/ERK activation increases JAK inhibitor efficacy in myeloproliferative neoplasms. *J Clin Invest*. 2019;129:1596-1611.
37. Lee S, Shah T, Yin C, et al. Ruxolitinib significantly enhances in vitro apoptosis in Hodgkin lymphoma and primary mediastinal B-cell lymphoma and survival in a lymphoma xenograft murine model. *Oncotarget*. 2018;9:9776-9788.

SUPPORTING INFORMATION

Additional supporting information may be found in the online version of the article at the publisher's website.

How to cite this article: Iwasaki T, Hayashi K, Matsushita M, et al. Merkel cell polyomavirus–negative Merkel cell carcinoma is associated with JAK-STAT and MEK-ERK pathway activation. *Cancer Sci*. 2022;113:251–260. https://doi.org/ 10.1111/cas.15187